Structure of Polyelectrolyte Solutions (Commemoration Issue Dedicated to Professor Hiroshi Ibagaki, Professor Michio Kurata, Professor Ryozo Kitamura, On the Occasion of Their Retirments)

AUTHOR(S):

Kaji, Keisuke; Kanaya, Toshiji; Urakawa, Hiroshi; Nishida, Koji; Kitamaru, Ryozo; Higgins, Julia S.; Gabry, Barbara

CITATION:

Kaji, Keisuke ...[et al]. Structure of Polyelectrolyte Solutions (Commemoration Issue Dedicated to Professor Hiroshi Ibagaki, Professor Michio Kurata, Professor Ryozo Kitamura, On the Occasion of Their Retirments). Bulletin of the Institute for Chemical Research, Kyoto University 1989, 66(3): 352-367

ISSUE DATE:

1989-02-15

URL:

http://hdl.handle.net/2433/77227

Bull. Inst. Chem. Res., Kyoto Univ., Vol. 66, No. 3, 1988

REVIEW

Structure of Polyelectrolyte Solutions

Keisuke KAJI*, Toshiji KANAYA*, Hiroshi URAKAWA*†,
Koji NISHIDA*, Ryozo KITAMARU*††, Julia S. HIGGINS**,
and Barbara GABRYŚ**†††

Received December 20, 1988

The structure of polyelectrolyte solutions was studied using X-ray and neutron scattering techniques. The phase diagram as a function of degree of polymerization and polymer concentration, which we constructed based on the wormlike-chain model, is first described. This diagram predicts dilute and semidilute regions; the former region is separated into two regimes, termed order and disorder, while the latter region is divided into at least three regimes, called isotropic, transition, and lattice in order of decreasing concentration. The structures of the isotropic and the lattice regimes were depicted theoretically by de Gennes et al., and that of the transition regimes was given by Odijk. The order and disorder regimes are distinguished from each other by whether or not an intermolecular single correlation due to electrostatic repulsive forces exists. Experimental evidence for the dilute-semidilute crossover concentration and the melting concentration between the isotropic and the transition regimes is also given. The static structures in the isotropic and transition regimes are discussed. Finally, the molecular motions of counterions and polyions, which were examined using the time-of-flight spectrometer and the spin-echo spectrometer at the Institut Max von Laue-Paul Langevin (ILL), Grenoble, are described.

KEY WORDS: Polyelectrolytes/ Phase Diagram/ Molecular Motions/ SAXS/ Neutron Scattering/

1. INTRODUCTION

Polyelectrolyte solutions are of great importance not only in practical uses, but also in understanding various biochemical mechanisms. Although a large number of studies from thermodynamical and electrochemical points of view have been reported[1–3], more direct investigations into the molecular structures and motions are scare, probably because of its complexity of the system and the difficulties in experimental methods.

In recent years some theoretical progress concerning the static and dynamic structures of polyelectrolyte solutions was made by the school of de Gennes[4–9] and it has become clear that scattering techniques such as neutron, X-ray, and light scattering are useful for the experimental study of these problems. In this paper we review the

* 梶　慶輔, 金谷利治, 浦川　宏, 西田幸次, 北丸竜三 : Laboratory of Fundamental Material Properties, Institute for Chemical Research, Kyoto Unviersity, Uji, Kyoto 611.
** Department of Chemical Engineering and Chemical Technology, Imperial College, London, SW7 2AZ, United Kingdom.
† Present Address: Faculty of Engineering and Design, Kyoto Institute of Technology, Matsugasaki, Sakyo-ku, Kyoto 606.
†† Present Address: Faculty of Science and Technology, Ryukoku University, Seta, Otsu, Shiga 520-21.
††† Present Address: Department of Physics, Brunel University, Uxbridge, Middlesex UB8 3PH, United Kingdom.

results of our studies on polyelectrolyte solutions by means of small-angle X-ray scattering (SAXS) and neutron scattering. We first describe the phase diagram of polyelectrolyte solutions as a function of the degree of polymerization and the concentration[10], and then discuss the structures in two regimes, isotropic and transition, of this phase diagram from the experimental results[11-13]. Finally, we present the molecular motions of counterions and polyions revealed by quasielastic neutron scattering techniques[14,15].

2. CHARACTERISTIC FEATURES OF FLEXIBLE POLYELECTROLYTES IN SOLUTION

Linear polyelectrolytes having many ionizable side groups along the chain skeleton are dissociated into polyions and counterions in aqueous solution. For dilute solutions the dissociated counterions are generally in either of four states: ions paired with side groups of polyions, ions condensed on polyions, ions bound by polyions and free ions. For semidilute solutions no free ions exist.

In the case of strong electrolytes which will be discussed here ion pairs are practically negligible, and the fraction of the condensed ions depends on the charge density of polyion, i.e., $1-1/z\lambda$ for $\lambda > z^{-1}$ where z is the valence of counterions, and λ is the reduced coupling constant defined by

$$\lambda = l_B/a = e^2/\varepsilon k T a \tag{1}$$

(Oosawa-Manning theory for condensation[2,3])

Here a is the distance between neighbouring dissociative groups on the polyion, l_B is the Bjerrum length which is defined as the contour distance between neighbouring charge groups when the electrostatic energy, $e^2/\varepsilon l_B$, between them is equal to the thermal energy kT, and ε is the dielectric constant of the solvent. In the case of vinyl polyelectrolytes used in our studies, 67% counterions are condensed on the polyions, and the remaining 33% counterions are distributed in the solution.

These condensed ions are not fixed on the sites of polyions but move from site to site along the polyion, so that the charges of polyions are considered to be neutralized uniformly by a fraction of condensed ions. The unneutralized charges of polyions play two roles; one is the effect of short-range repulsive forces to extend polyion chains and the other is the effect of long-range repulsive forces to increase the excluded volume of polyion chains. Uncondensed counterions screen the intra- and interpolyion electrostatic repulsive forces to an extent depending on their concentrations. Therefore, the polyions behave as rods when the concentration is sufficiently low, whereas at high concentrations they assume coiled structures as neutral polymers. Because of such complex properties their structures change in various ways.

3. PHASE DIAGRAM

Fig. 1 shows the phase diagram as a function of the degree of polymerization N and the polymer concentration C for the aqueous solutions of vinyl polyelectrolytes at

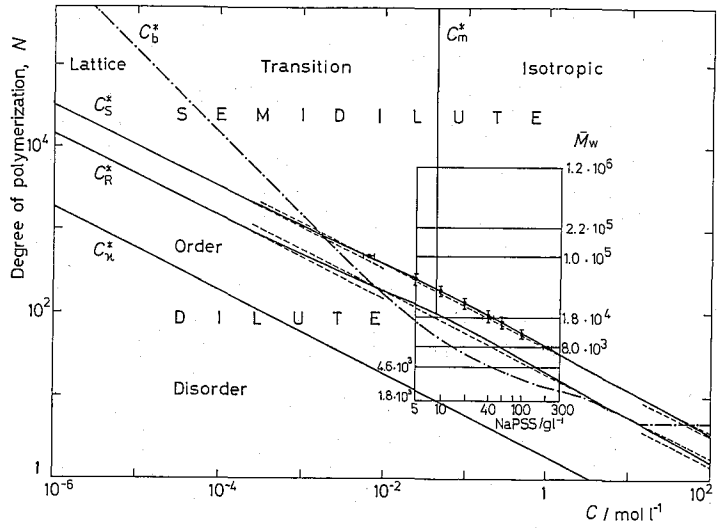

Fig. 1. Phase diagram for vinyl polyelectrolyte solutions as a function of the degree of polymerization N and the concentration C at ambient temperature.[10] The crossover lines and regimes are explained in the text. The area enclosed with a square is the region where the SAXS measurements were made for NaPSS solutions.

ambient temperature[10], which we constructed based on the theories of de Gennes et al.[4] and Odijk[6] by employing the wormlike-chain model. For this model the polyion size can be described by two parameters, a contour length l and a total persistence length b_t. In the case of polyelectrolytes b_t may be defined as the sum of electrostatic b_e and intrinsic b_o components: $b_t = b_e + b_o$. Compared with b_e, b_o may be neglected unless the concentration is very high since its value is of the order of 10Å for usual flexible polyelectrolytes, e.g., $b_o = 12$Å for sodium poly(styrene sulfonate). The concentration dependence of b_e was calculated numerically by Le Bret[9].

The polyion size is given by the mean-square end-to-end distance

$$\langle R^2 \rangle = 2b_t^2(\alpha - 1 + e^{-\alpha}) \tag{2}$$

or by the radius of gyration

$$\langle S^2 \rangle = b_t^2[\alpha/3 - 1 + (2/\alpha^2)(\alpha - 1 + e^{-\alpha})] \tag{3}$$

where $\alpha = 1/b_t$. The dilute-semidilute crossover concentrations for these sizes are calculated as follows:

$$C_R^* = N/(4/3)\pi(\langle R^2 \rangle^{1/2}/2)^3 \tag{4}$$

for the end-to-end distance, and

$$C_S^* = N/(4/3)\pi\langle S^2 \rangle^{3/2} \tag{5}$$

for the radius of gyration. However, scattering techniques such as X-ray, neutron, and light scattering cannot detect C_R^*, but only C_S^*.

In the semidilute region several regimes, lattice, transition, isotropic, and blob, were

defined by de Gennes et al.[4] and Odijk[6]. When $b_t \geq l$, the polyions become rodlike to form a lattice structure because of the strong electrostatic inter-rod interactions. The crossover concentration C_b^* at $b_t = l$ can be directly calculated from the concentration dependence of b_e given by Le Bret[9]. When $C > C_b^*$ or $b_t < l$, the lattice is deformed to an extent depending on the concentration, and at a critical concentration C_m^* it melts completely. The melting concentration is determined from the Lindemann rule[6] that melting occurs if the ratio of the mean-square displacement of the polyions to the inter-rod distance exceeds a certain value~0.15. Above C_m^* the polyions are coiled and overlapped with one another; they are however different from neutral polymers in semidilute solution in having correlation holes due to intermolecular electrostatic repulsive forces. This structure was visualized by de Gennes et al.[4] and called isotropic. The blob regime predicted by Odijk[6] would appear above a concentration range of the isotropic regime. The dilute region is also distinguished into order and disorder regimes, the crossover C_κ^* between which is estimated as a concentration where the electrostatic screening length κ^{-1} is equal to half the distance between two neighbouring polyion centers.

4. CONFIRMATION OF C_S^*

The dilute-semidilute crossover concentration C_S^* for the radius of gyration can be detected by various experimental methods. We confirmed this using the SAXS method. The SAXS intensity curves of the polyelectrolyte solutions show a single correlation peak, and the maximum position Q_m of this peak depends on the polymer concentration C as shown in Fig. 2, where Q is defined by $4\pi \sin\theta/\lambda$ as usual. It is

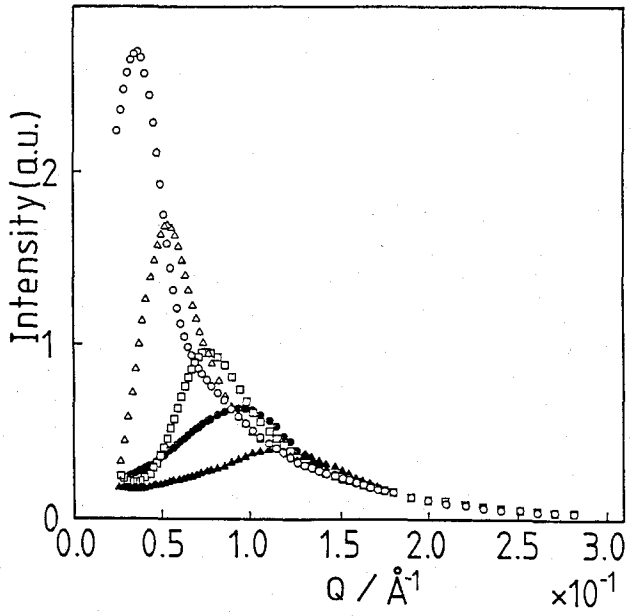

Fig. 2. The concentration dependence of SAXS curves for NaPPS, $M_w = 1.0 \times 10^5$.[10] $C/\mathrm{gl}^{-1} = 10(\bigcirc)$, $20(\triangle)$, $40(\square)$, $60(\bullet)$, and $100(\blacktriangle)$.

predicted from the theories that $Q_m \sim C^{1/2}$ in the semidilute region whereas $Q_m \sim C^{1/3}$ in the dilute order regime. The crossover concentration C_S^* can be therefore determined experimentally as an inflection point from $C^{1/2}$ to $C^{1/3}$ in the log-log plot of Q_m vs C. Fig. 3 shows such plots for sodium poly(styrene sulfonate)(NaPSS) having various molecular weights M_w. The relation $Q_m=0.17\ C^{1/2}$ is for the semidilute solutions and most of observed Q_m values fall on this line, independently of M_w. The observed Q_m values for the dilute solutions agree well with the relation $Q_m \sim C^{1/3}$ except for the lowest M_w. The crossover concentrations obtained from Fig. 3 and from other relations such as $Q_m - C/N$ and $Q_m - N$ plots are also shown in Fig. 1 where N is degree of polymerization. They confirm the C_S^* within a concentration range $10^{-2} \simeq 1$ mol/l.

This crossover line C_S^* has also been confirmed in a wider concentration range

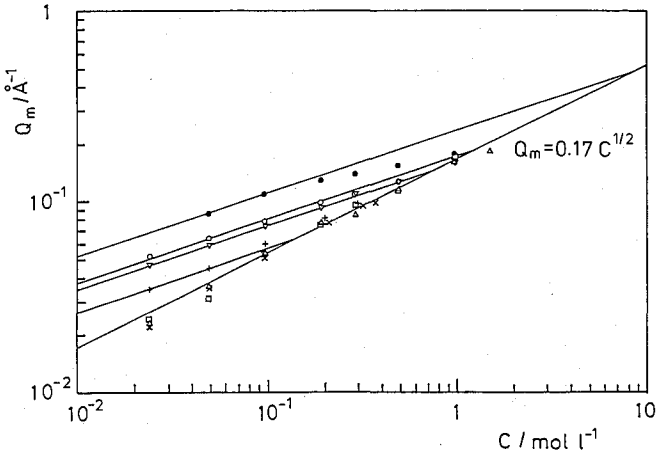

Fig. 3. The Q_m-C plot for NaPSS solutions.[10] $Q_m=0.17C^{1/2}$ indicates the observed relation for semidilute solutions. $M_w=1.8\times10^3$(●), 4.6×10^3(○), 8.0×10^3(▽), 1.8×10^4(+), 1.0×10^5(△), 2.2×10^5(×), and 1.2×10^6(□).

$10^{-4} \sim 3$ mol/l by a dynamic method. Ito et al[17] revealed that the high frequency dielectric relaxation (MHz in order of magnitude) is caused by the fluctuation of loosely bound counterions in the direction normal to the polyion axis, this motion being termed plasmon. The dielectric increment $\Delta\varepsilon$ and the relaxation time τ show different behaviour in the dilute and the semidilute regions. The crossover concentrations obtained from the measurements of $\Delta\varepsilon$ and τ agree surprisingly well with the C_S^* presented in Fig. 1.

5. STRUCTURE OF THE ISOTROPIC REGIME

De Gennes et al.[4] pictured the structure of this regime; polyions are entangled to form an isotropic system where the intersegmental electrostatic repulsive forces between neighbouring entangled points make correlation holes. This correlation length ξ is independent of molecular weight, and the segments within the distance ξ are nearly

stiff, whereas the chains as a whole are random coils.

We investigated the structure of this regime by the distance distribution analysis of SAXS curves. In order to separate the effect of counterions, SAXS measurements were carried out for poly(vinyl hydrogen sulfate) or a sulfuric acid ester of poly(vinyl alcohol)[$-CH_2CH(OSO_3H)-$]$_n$ and its Li, Na, and K salts, which are designated HPVS, LiPVS, NaPVS, and KPVS, respectively. The samples having the average degree of polymerization $P=1500$ and the degree of esterification $\alpha=96\%$ were solved in deionized water to provide 0.2 monomer mol/l aqueous solutions. Fig. 4 shows the observed SAXS curves of these samples after correction. Every curve shows a single peak and all the profiles are similar. The peak intensity however increases with increasing number of electrons in the counterions. The scattering of HPVS corresponds to that of the polyions themselves without counterions because protons having no electrons do not contribute to the scattering. Judging from these features, it is expected that there exist nearest-neighbour correlations in the solution, and the difference in intensity is due to that in contrast between the polyions on which 67% counterions are condensed and the solvent including the remaining uncondensed counterious. To confirm these predictions, we calculated distance distribution functions $P(r)$ from the SAXS curves by the inverse Fourier transformation:

$$P(r)=4\pi r^2\gamma(r) \tag{6}$$

where $\gamma(r)$ is a correlation function. The results are shown in Fig. 5. The line $P(r)=$

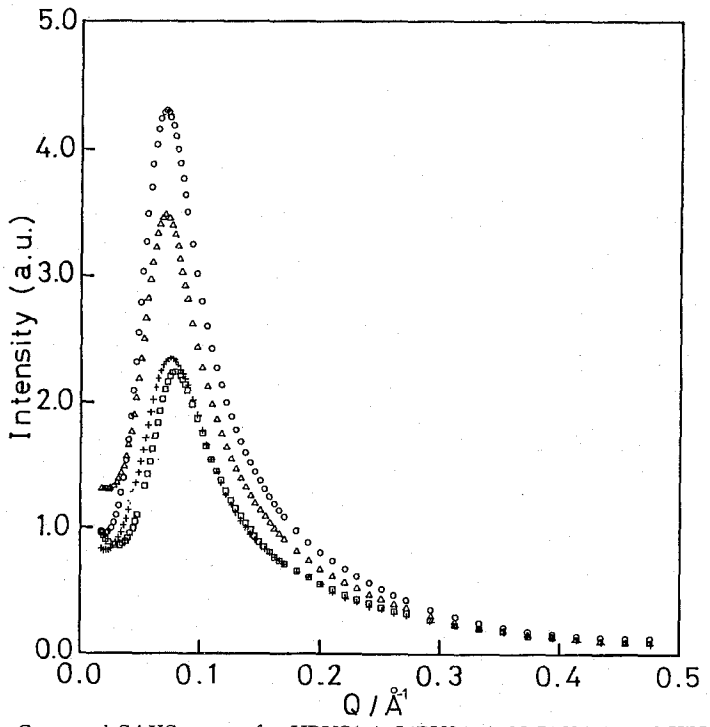

Fig. 4. Corrected SAXS curves for HPVS(□), LiPVS(+), NaPVS(△), and KPVS(○).[12]

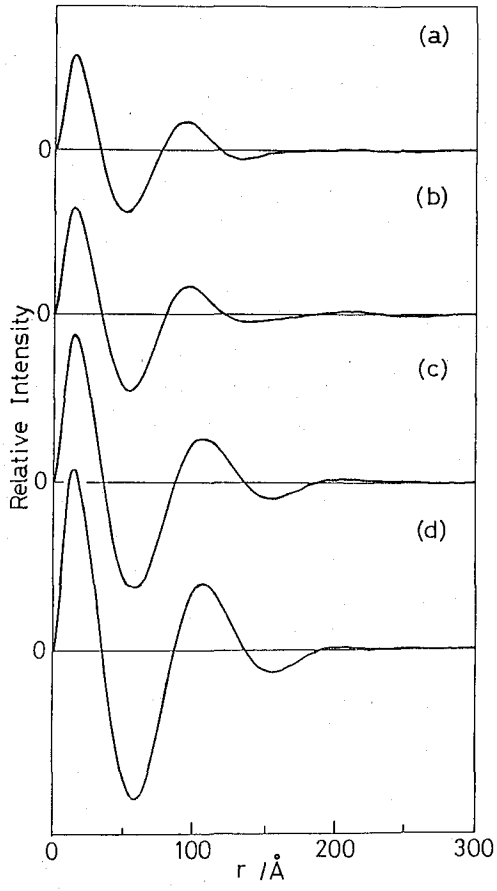

Fig. 5. Distance distribution functions for the semidilute solutions of HPVS(a), LiPVS(b), NaPVS(c), and KPVS(d).[12]

0 corresponds to the average distance distribution density over the total solution system. Every $P(r)$ function has two peaks in the range 0–300Å; the first peak is considered to be related to intrasegmental correlations. The maximum position of this peak, however, does not mean any characteristic correlation length since due to a weighting factor $4\pi r^2$, $P(r)$ is deformed from $\gamma(r)$ which has its maximum intensity at $r=0$. The second peak is presumed to be due to intersegmental correlations because a deep negative correlation well exists between the first and second peaks. The negative correlation corresponds to the presence of regions having lower density than the average, which are called correlation holes. However, no higher-order peaks having appreciable intensity are seen. This provides evidence that the structure of the solution can be well described by a nearest-neighbour correlation model, which is a feature of the isotropic model, as schematically shown in Fig. 6. The nearest-neighbour correlation model can also explain the slight shift of the maximum position of the second correlation peak with couterion species. The intersegmental correlation lengths ξ are listed in Table 1, together with the radii of the polyion cross-sections r_0, estimated from the slopes in a high Q range of the SAXS curves. The difference in ξ between HPVS and KPVS, for example, is 13Å, which is almost double of the sum of the $r_0=5.1$Å for HPVS and the

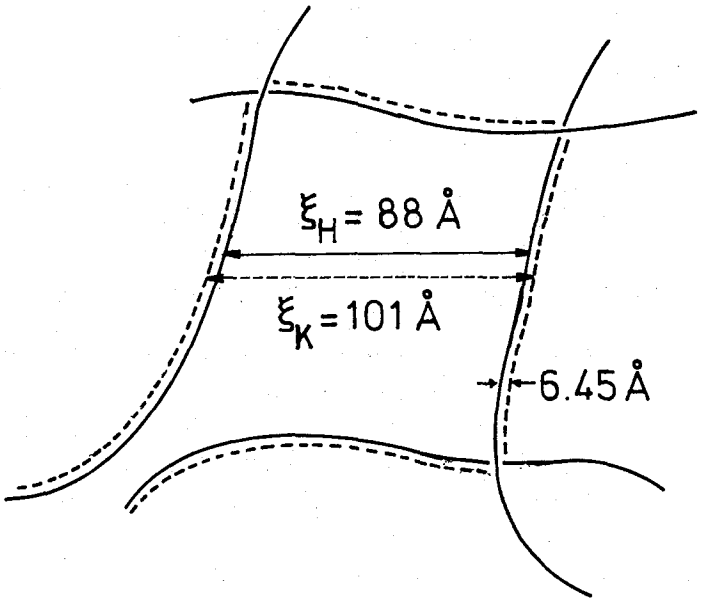

Fig. 6. Nearest-neighbour correlation model for the isotropic regime. Solid and broken curves denote the lines of maximum electron density in HPVS and KPVS chains, respectively. ξ_H and ξ_K are their correlation lengths.

Table 1. Intersegmental correlation lengths ξ and radii of polyion cross-section r_0 of HPVS and its Li, Na, and K salts estimated from the SAXS curves. The polymer concentration 0.2 monomer mol/l, the average degree of polymerization $P\simeq1500$, and the degree of esterification $\alpha=96\%$.

Polyelectrolyte	ξ/Å	r_0/Å
HPVS	88	5.1±0.3
LiPVS	90	5.2±0.3
NaPVS	100	5.9±0.4
KPVS	101	6.1±0.4

raduis of the counterion K^+(1.35Å). This may support the nearest-neighbour model if the charged side groups between the nearest-neighbour segments are assumed to orient to the opposite direction because of electrostatic repulsions.

Small-angle neutron scattering (SANS) measurements were carried out[13] to make clear that the first peak in $P(r)$ is due to the intrasegmental correlations, so that the intersegmental correlation function is negative within a range zero to ξ. The total scattering function $S(Q)$ is the sum of the intramolecular scattering function $S_1(Q)$ and the intermolecular one $S_2(Q)$:

$$S(Q)=S_1(Q)+S_2(Q) \tag{7}$$

The SANS measurements by means of deuterium labeling can separate these two parts. When the fraction of D-polymer is designated as x, the total scattering function of the system where H-polymer is invisible to neutrons can be given by

$$S_x(Q)=xS_1(Q)+x^2S_2(Q). \tag{8}$$

Plotting $S_x(Q)/x$ against x at a given Q provides a straight line; the intersection at $x=0$ and the slope correspond to $S_1(Q)$ and $S_2(Q)$, respectively. In this study a system of hydrogenated and deuterated NaPVS dissolved in a D_2O/H_2O mixture, which was adjusted to match the scattering length density of the hydrogenated NaPVS, was used, and x was taken to be 0.25, 0.50, 0.75, and 1.0. From similar plottings for various values of Q, the Q dependence of their scattering functions can be obtained. The results are shown in Fig. 7. The scattering function of a single chain $S_1(Q)$ corresponds to that of a rod within the observed Q range, and the intermolecular scattering function $S_2(Q)$ is negative. The inverse Fourier transformation of $S_2(Q)$ gives a deep correlation hole within a scale of ξ, which does not contain the intramolecular correlation peak.

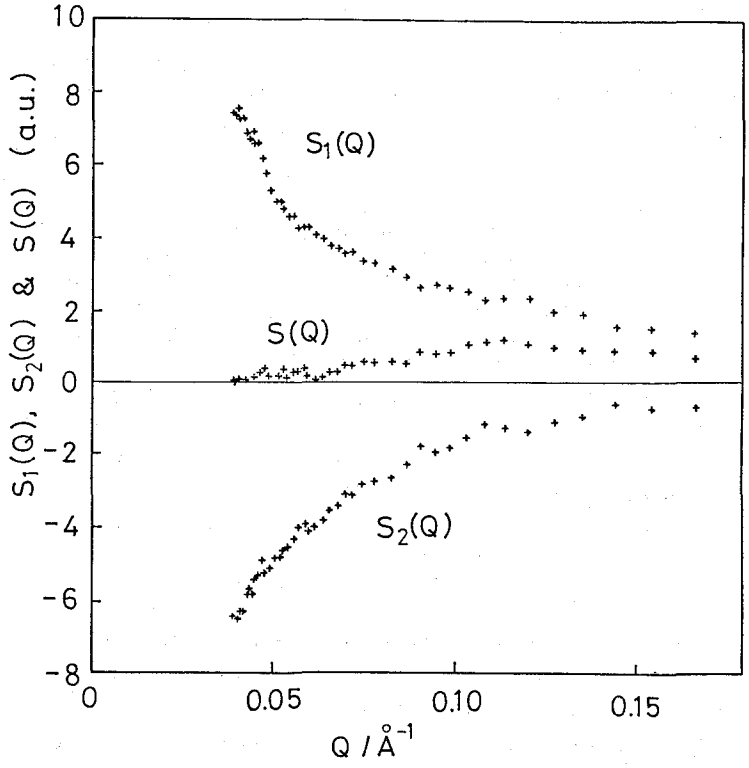

Fig. 7. Separation of the total scattering function, $S(Q)$, of NaPVS solution into intra- and intermolecular ones, $S_1(Q)$ and $S_2(Q)$.[13] The polymer concentration is 0.7 mol/l.

6. STRUCTURE IN THE TRANSITION REGIME

As described in Section 3, the structure of the polyelectrolyte solution changes at

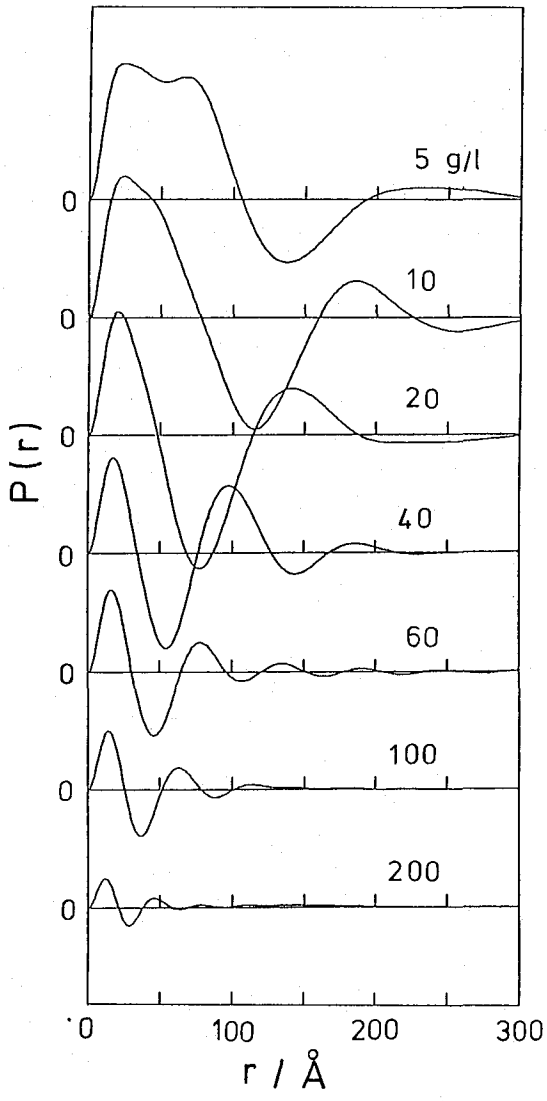

Fig. 8. Distance distribution functions $P(r)$ for various concentrations of NaPSS solutions.[11] $M_w=1\times10^5$.

the melting crossover concentration C_m^*, below which the transition regime appears. In this section we will show how the existence of C_m^* was experimentally confirmed and what the structural feature of this regime is[11].

For these purposes, we examined sodium poly(styrene sulfonate)(NaPSS) solutions around C_m^* by distance distribution analysis of their SAXS curves. The polymer concentration C and the molecular weight M_w were changed within ranges between 5 and 200 g/l and between 1800 and 1.2×10^5, respectively. A typical example of obtained $P(r)$ functions for $M_w=1\times10^5$ is shown in Fig. 8. Every curve has the intra- and intersegmental correlation peaks. The maximum position of the intersegmental nearest-neighbour correlation peak increases proportional to $C^{-1/2}$ as was shown in section 4. The intrasegmental peak however exhibits an anomalous change; it is broadened with decreasing concentration and becomes first a peak with a shoulder and

then a doublet. As the lithium salt of this polyelectrolyte still gives almost the same $P(r)$, this change is not due to a regular array of bound counterions, but due to polyion chain conformation itself. The broadening of this peak may be explained in terms of the increase of the persistence length of the polyion. The appearance of a new peak however indicates the formation of some regular chain conformation. Further, it occurs below $C_m^* \simeq 10$ g/l, but never appears for molecular weights below $M_w = 18{,}000$. Thus, the appearance of the new peak corresponds to the transition regime in Fig. 1, because when M_w is less than 18,000, the solution of concentrations below C_m^* is in the dilute region. Conversely, the above results support the C_m^* of the phase diagram of Fig. 1.

As a possible regular conformation of the polyion in the transition regime, we proposed an electrostatic helix model, which is schematically shown in Fig. 9. In this model the pitch, $P = 75$Å, of the helix corresponds to the maximum position of the new peak. Because of the large pitch and strong electrostatic repulsive forces it seems that the tacticity of the polyion does not affect the helix stucture.

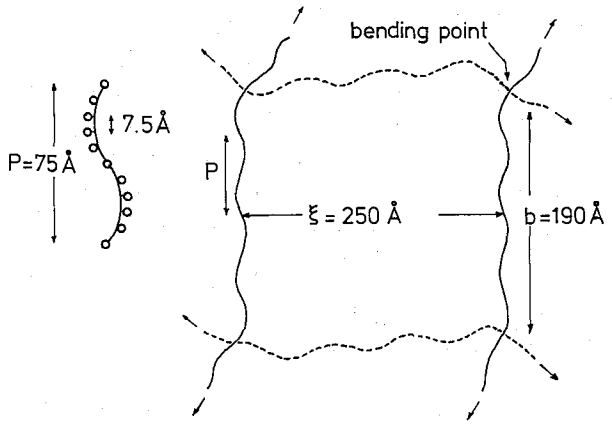

Fig. 9. Electrostatic helix model for the transition regime. The figures are for the case when $C \simeq C_m$. P:pitch of the helix, ξ:correlation length, and b:persistence length, open circle: charged side group.

7. MOTIONS OF COUNTERIONS

As already described, 67% counterions are condensed on polyions and the remaining 33% counterions are distributed in the solution. The uncondensed counterions are bound by polyions and oscillate cooperatively with a frequency in MHz around the polyion chain axis, in what is called a plasmon. The condensed counterions migrate from one end to the other end of the polyion, so that this frequency depends on the contour length of the polyion, but in the case of usual molecular weights the frequency is in the order of kHz. These two modes have been detected by Hayakawa et al.[17] using dielectric relaxation method. However, the motion of the counterions condensed on the fixed sites was not detected because it is very fast. Such a motion can be detected using a quasielastic neutron scattering method. We examined the motion of

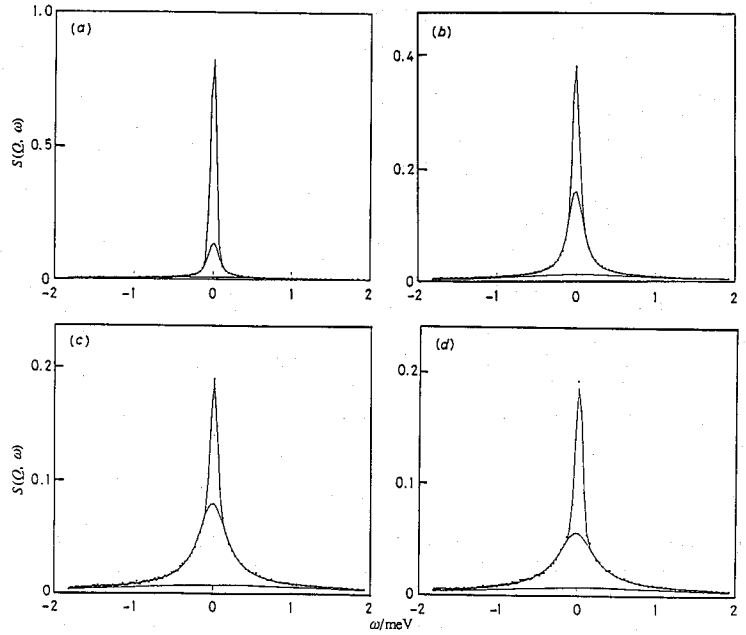

Fig. 10. An example of the scattering law $S(Q, \omega)$ for the D_2O solution of PVS-d_3-TMA [$-CD_2-CD(-OSO_3^-N^+(CH_3)_4)-$].[14] Here $Q/Å^{-1}$=0.40(a), 0.80(b), 1.20(c), and 1.60(d).

tetra-methyl ammonium(TMA) ions as counterions[14]. To remove the contribution from polyions, deuterated poly(vinyl sulfate)(D-PVS) was used because the incoherent scattering cross-section of H is very large compared with that of other atoms such as D, C, O, and S, i.e., the neutron scattering sees only the motion of H atoms. The measurements were carried out using a time-of-flight spectrometer(IN6) at ILL, Grenoble. Fig. 10 shows an example of the Q-dependence of energy spectra $S(Q, \omega)$ for the sample of concentration 0.25 mol/l. The abscissa is the energy shift $\hbar\omega$ of scattered neutrons, and at $\hbar\omega=0$ elastic scattering occurs. These spectra were decomposed into three components, one elastic and two quasielastic parts, and analysed with the elastic incoherent structure factor (EISF), defined by

$$EISF = I_e(Q)/[I_e(Q)+I_q(Q)] \tag{9}$$

where $I_e(Q)$ and $I_q(Q)$ are the integrated intensities of the elastic and the quasielastic scattering components, respectively. The Q-dependence of the observed $EISF$ was well-described using a three-fold circular-jump model accompanied by damped vibrations. The comparsion of this model with the observed results is shown in Fig. 11, which shows a good agreement. This model visualizes the motion of condensed TMA ions at binding sites by assuming that the TMA ion has a tetrahedral structure and its binding site is either of the four faces of the tetrahedron. The axis of the jump rotation at a given binding-site is the three-fold axis of the tetrahedron, so that there are three jump-sites. The jump frequency and the frequency of the damped vibration at each jump-site were estimated to be 10^{13} and 10^{12} Hz, respectively, from the widths of two quasielastic components.

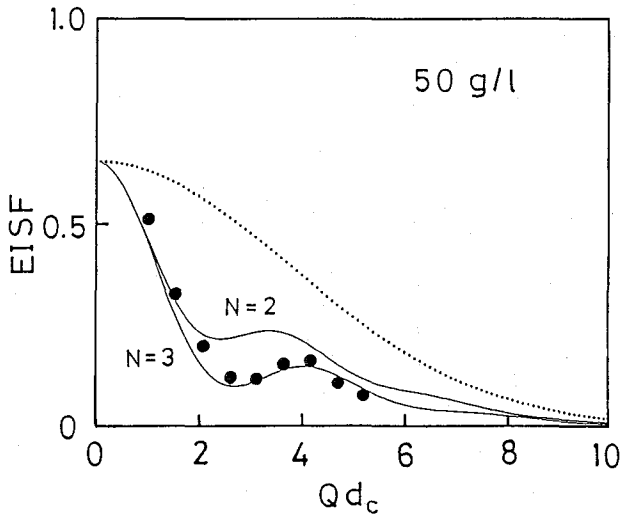

Fig. 11. Comparison of the *EISF* calculated for the circular-jump model (solid curves) and the experimental values (solid circles).[14] C=50 g/dm^3, the radius of the circle d_c=2.6Å. The dotted line denotes a damping factor.

8. MOTIONS OF POLYIONS

It is expected that the motions of polyions are different in the dilute and the semidilute regions, so that the crossover concentration between them can be also detected by dynamic measurements. To confirm this expectation, we carried out a neutron spin-echo study of NaPSS solutions, using the spin-echo spectrometer(IN11) at ILL, Grenoble[15]. The experiments were carried out as a function of molecular weight at a fixed polymer concentration 76 g/l. The spectrometer provides the intermediate scattering law or the time correlation functions $I(Q, t)$. An example of the observed $I(Q, t)$ is shown in Fig. 12. These correlation functions can be described by a single exponential function normalized to unity at t=0 or by $\exp(-t/\tau(Q))$ where $\tau(Q)$ is a

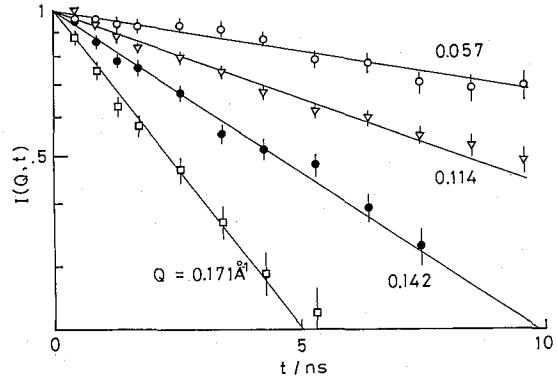

Fig. 12. Time correlation functions for NaPSS, DP=5790, in the solution of C=76g/l at various Q values.[15] Solid lines are best fits of a function $\exp(-t/\tau(Q))$.

Q-dependent correlation time. Using $\tau(Q)$, the Q-dependent effective diffusion coefficient is defined by

$$D_{\mathrm{eff}}(Q)=\tau^{-1}(Q)/Q^2 \tag{10}$$

In Fig. 13, the obtained $D_{\mathrm{eff}}{}^{-1}(Q)$ values are plotted as a function of Q, together with the static structure factors $S(Q)$ also measured on IN11. For $DP \geqq 87$, $D_{\mathrm{eff}}{}^{-1}(Q)$ shows a broad peak at $Q_{\mathrm{m}}=0.11\text{Å}^{-1}$ being around the peak position of $S(Q)$. This

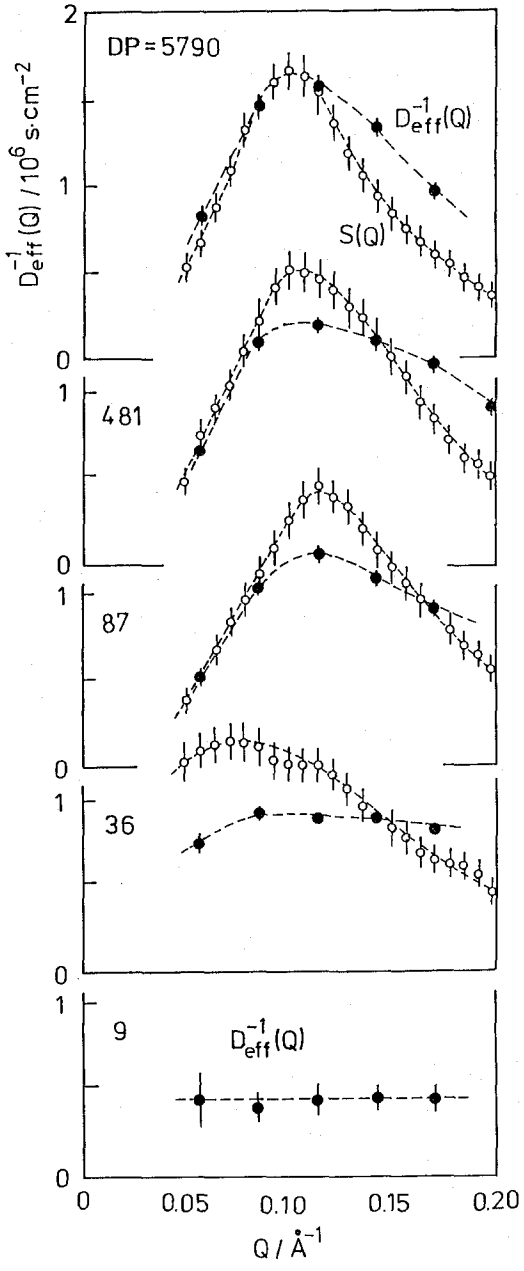

Fig. 13. Inverse of the effective diffusion coefficient $D_{\mathrm{eff}}{}^{-1}(Q)$(●) and the static structure factor $S(Q)$(○) for NaPSS solutions.[15]

strongly supports the argument that the electrostatic interactions between polyion segments are repulsive. For $DP \leqq 36$, however, $D_{\mathrm{eff}}^{-1}(Q)$ is almost independent of Q, especially for $DP=9$, which suggests that short polyions are in the dilute region and their diffusion obeys a simple diffusion theory; the influence of the electrostatic interactions on the diffusion is negligible in this case.

To obtain the dilute-semidilute transition point, $D_{\mathrm{eff}}(Q)$ was plotted as a function of DP at $Q=0.114\text{Å}^{-1} \simeq Q_{\mathrm{m}}$. The results are shown in Fig. 14. For the high DP samples, $D_{\mathrm{eff}}(Q)$ is almost independent of DP, which is predicted in the semidilute region. For the low DP samples, however, it increases rapidly with decreasing DP. The latter DP dependence was described by the translational diffusion of a prolate ellipsoid as a short fully extended polyion. From the crossover point of the former and the latter relations, we obtained the transition DP^* from the dilute to the semidilute region. This DP^* agrees very well with the dilute-semidilute crossover line C_S^* in Fig. 1 at $C=76$ g/l.

In conclusion we would like to emphasize that the phase-diagram in Fig. 1 is of great importance as a basis for study of both the static and dynamic structure of polyelectrolyte solutions.

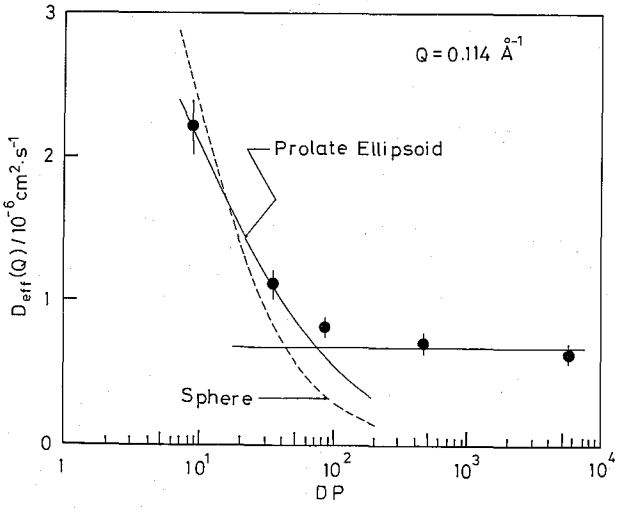

Fig. 14. Molecular-weight dependence of the effective diffusion coefficient $D_{\mathrm{eff}}(Q)$ at $Q=0.114\text{Å}^{-1}$.[15] Solid and dashed curves are the calculated results for a prolate ellipsoid and a sphere having the same radius of gyration.

REFERENCES

(1) S. A. Rice and M. Nagasawa, "Polyelectrolyte Solutions", Academic Press, New York, 1961.
(2) F. Oosawa, "Polyelectrolytes", Marcel Dekker, New York, 1971.
(3) E. Selegny, M. Mandel, U. Strauss (editors), "Polyelectrolytes", D. Reidel, Dordrecht, 1974.
(4) P. G. de Gennes, P. Pincus, R. M. Velasco, and F. Brochard, *J. Physique*, **37**, 1461 (1976).
(5) C. E. Williams et al., *J. Polym. Sci. Polym. Lett. Ed.*, **17**, 379 (1979).

(6) T. Odijk, *Macromolecules*, **12**, 688 (1979).
(7) J. Hayter, G. Jannink, F. Brochard, and P. G. de Gennes, *J. Physique-Lett.*, **41**, L-451 (1980).
(8) M. Drifford and J.-P. Dalbiez, *J. Phys. Chem.*, **88**, 5368 (1984).
(9) M. Nierlich, et al., *J. Physique*, **46**, 649 (1985); *Colloid & Polym. Sci.*, **263**, 955 (1985).
(10) K. Kaji, H. Urakawa, T. Kanaya, R. Kitamaru, *J. Phys. France*, **49**, 933 (1988).
(11) H. Urakawa, K. Kaji, T. Kanaya, R. Kitamaru, IUPAC Macro 88 Preprints, 1988, p. 295.
(12) K. Kaji, H. Urakawa, T. Kanaya, R. Kitamaru, *Macromolecules*, **17**, 1835 (1984).
(13) M. Ono, S. Okamoto, T. Kanaya, K. Nishida, H. Urakawa, K. Kaji, R. Kitamaru, *Physica*, **138B**, 49 (1986).
(14) T. Kanaya, K. Kaji, R. Kitamaru, B. Gabryś, J. S. Higgins, *J. Chem. Soc. Faraday Trans.* 1, **84**, 3487 (1988).
(15) T. Kanaya, K. Kaji, R. Kitamaru, J. S. Higgins, B. Farago, *Macromolecules*, **22** (1989) in press.
(16) For example, see H. Yamakawa, "Modern Theory of Polymer Solutions", Harper & Row, New York, 1971.
(17) K. Ito, N. Ookubo, R. Hayakawa, *Rep. Prog. Polym. Phys. Jpn.*, **29**, 83 (1986); K. Ito, A. Yagi, N. Ookubo, R. Hayakawa, *ibid.*, **29**, 87 (1986).